ADVANCED MATERIALS

DOI: 10.1002/adma.200702382

Size-Controlled *Ex-nihilo* Ferromagnetism in Capped CdSe Quantum Dots

By *Mohindar S. Seehra,* Prasanta Dutta, Sonnathi Neeleshwar, Yang-Yuan Chen,* Cheng Lung Chen, Shang Wei Chou, Chia Chun Chen, Chung-Li Dong,* and *Ching-Lin Chang*

The potential of exploiting the spin of the electron (in addition to its charge) in novel new electronic devices and the associated opportunities for new science has led to extensive search for viable magnetic semiconductors with room temperature ferromagnetism (RTFM).[1–3] Some success for ferromagnetism has been reported in dilute magnetic semiconductors (DMS) and dilute magnetic oxides (DMO) containing a few percent of transition metal ions such as (Ga,Mn)As,[4,5] (Zn,M)O[6–9], and (Ti,M)O_2[10–12] with M = V, Cr, Mn, Co, Ni, and Cu. Despite the numerous reports on the successful observation of room temperature ferromagnetism (RTFM) in a number of these systems in apparent agreement with computations based on density functional theory, the issue remains unsettled and contentious for a number of reasons including lingering doubt of the possible role of undetected ferromagnetic impurities such as Fe, Co, and Ni. In some systems such as (Zn,Ni)O[13] and (Zn,Cr)Te[14] the observed RTFM has been linked to clustering of Ni and Cr nanocrystals, respectively.

In this paper, we report the observation of RTFM in CdSe quantum dots (QD) capped with TOPO (tri-*n*-octylphosphine oxide). This RTFM is labeled as *ex-nihilo* since the RTFM is due to the marriage of two diamagnetic materials viz. CdSe and TOPO, possibly resulting from charge transfer from Cd d-band to the oxygen atoms of TOPO. We further show that the RTFM varies inversely with the size of the QD, in agreement with our calculations.

CdSe is a II-VI semiconductor with direct band gap $E_g = 1.74$ eV at 300 K. Semiconductors nanocrystals (NCs) such as CdSe are often called quantum dots (QD) when the size of the first Bohr radius exceeds the crystallite size D, leading to quantum confinement effects such as increase in the band-gap E_g with decrease in D. For the CdSe NCs, E_g can be tuned to cover the whole visible range by change in D, thus making this system potentially useful for solar energy applications.[15,16] Attempts to dope CdSe with Mn to obtain a magnetic semiconductor have not been successful partly because of the limited solubility of Mn in CdSe. However, Magana et al. have reported superparamagnetism with a blocking temperature $T_B \simeq 40$ K in thermally annealed Mn/CdSe QD's.[17]

As the size of the nanocrystals is decreased, the fraction of atoms on the surface to the total number of atoms in NC increases as $1/D$. Since the atoms on the surface experience broken symmetry and often higher anisotropy, new surface states are formed. For the CdSe QDs, a number of interesting optical properties such as band edge luminescence[18] and excitonic radiative decay[19] have been related to the surface states. Since CdSe NCs are often passivated by capping with TOPO (tri-*n*-octylphosphine oxide) to avoid aggregation and surface oxidation, it is important to understand the effect of TOPO on the surface atoms and on the measured properties. XPS[15] and EXAFS[20] studies on TOPO passivated CdSe QDs have shown that TOPO binds only at the Cd site and that the surface coverage on the Cd sites varies from a high of about 60% for $D = 2$ nm to about 35% for $D > 3$ nm. This incomplete coverage results from the stereochemistry of the large TOPO molecule $[CH_3(CH_2)_7]_3PO$ with MW = 386.64.

In CdSe QDs, we report here the observation of size-dependent RTFM whose strength, with increase in size D of the QDs, weakens as measured by the saturation magnetization M_s and intensity of the electron magnetic resonance (EMR) line. As noted earlier, we associate this ferromagnetism with 4d holes on TOPO-coated Cd surface atoms generated through charge transfer to TOPO via the surface Cd–TOPO bonds, yielding 0.0075 μ_B/Cd surface atom bonded to TOPO. In support of this claim and to rule out Fe-based impurities as the source of this magnetism, the following arguments are presented: (i) All the samples of CdSe QDs with $D = 1.8$, 2.8, 4.1, 5.6, and 7.0 nm are prepared using the same procedures and the same sources for the chemicals used for synthesis (see details under Experimental). ICP-AES (Inductively Coupled Plasma-Atomic Emission Spectroscopy) analysis of the samples limit the Fe content of the samples to be less than 0.1 ppm, the precision of this technique. This

[*] Prof. M. S. Seehra, Dr. P. Dutta
Department of Physics, West Virginia University
Morgantown, WV 26506 (USA)
E-mail: mseehra@wvu.edu
Dr. Y.-Y. Chen, Dr. C. L. Chen, Dr. C.-L. Dong
Institute of Physics, Academia Sinica
Taipei, Taiwan (Republic of China)
E-mail: cheny2@phys.sinica.edu.tw
Dr. S. Neeleshwar
University School of Basic and Applied Sciences, G. G. S. Indraprastha University
Kashmere Gate, Delhi (India)
Dr. S. W. Chou, Dr. C. C. Chen
Department of Chemistry, National Taiwan Normal University
Taipei, Taiwan (Republic of China)
Dr. C.-L. Chang
Department of Physics, Tamkang University
Tamsui 251, Taiwan (Republic of China)

WILEY InterScience DISCOVER SOMETHING GREAT
© 2008 WILEY-VCH Verlag GmbH & Co. KGaA, Weinheim

magnitude of Fe or its oxides, if present, would yield M_s values at least two orders of magnitudes smaller than the observed value; (ii) The decrease of M_s with increase in size D of the QD, with the corresponding effect on the intensity of the EMR line, is difficult to explain in terms of impurity; (iii) Direct evidence of size-dependent charge transfer from Cd to TOPO in our samples is presented using EXAFS. These results of size-dependent ferromagnetism are very intriguing because bulk CdSe is a diamagnet with magnetic susceptibility $\chi_d = -2.25 \times 10^{-7}$ emu $g^{-1}Oe^{-1}$.[16]

The hysteresis loop data for the 1.8 nm sample at 5 K and 300 K are shown in Figure 1a. The raw data was corrected for the diamagnetic contribution from the high field regions. The diamagnetic-corrected magnetization is essentially saturated above 10 kOe and the coercivity H_c decreases with increase in temperature. The temperature variations of H_c, the remanence M_r (for $H = 0$) and the saturation magnetization M_s for $D = 1.8$, 2.8, and 4.1 nm are shown in Figure 1b. For the smallest 1.8 nm sample, the relatively large magnitudes of M_s, M_r and H_c in Figure 1b even at 370 K are evidence of ferromagnetism with $T_c > 370$ K. For the larger 4.1 nm sample, the magnitudes of M_r and M_s at 300 K are considerably smaller but not zero. Temperatures higher than 370 K were not accessible with the present configuration of the SQUID (Superconducting Quantum Interference Device) magnetometer used in these studies.

The standard first derivative EMR spectra for the 1.8, 2.8, 4.1, 5.6, and 7 nm samples at room temperature are shown in Figure 2a. There is no noticeable EMR signal for the 5.6 and 7 nm samples and only a weak signal for the 4.1 nm sample. For the 1.8 and 2.8 nm samples, there is only a small shift of the resonance field H_0 and the linewidth ΔH with temperature (see Fig. 2b for the 1.8 nm sample), a result expected for a ferromagnet with $T_c > 370$ K. However, there is a more noticeable shift of H_0 with change in size D, H_0 decreasing as D decreases (Fig. 2a). This can be understood from the condition for resonance in the presence of anisotropy field H_A: $(hf/g\mu_B) = H_0 + H_A$, where h is the Planck's constant, $g \backsimeq 2$ for a free electron and $f = 9.28$ GHz is the fixed operating frequency. The data in Figure 3b suggests increase in anisotropy H_A with decrease in size D, a result qualitatively understandable in terms of the reduced symmetry of surface atoms responsible for the EMR signal, and hence higher anisotropy.

The variation of the saturation magnetization M_s for our samples versus $1/D$ is shown in Figure 3a. We used these values of M_s to determine magnetic moment μ associated with each surface Cd atom bonded to TOPO using the following analysis. The lattice parameters of $a = 4.299$ Å, $c = 7.01$ Å, volume $a_0^3 = 3^{1/2} a^2 c/2$ with $a_0 = 4.823$ Å of the unit cell with two CdSe units/cell, and density $\rho = 5.665$ g cm^{-3} were used to calculate the number of surface atoms for spherical particles of diameter D. It was further assumed that Cd and Se have equal numbers of atoms on the surface with average separation of a_0. Using the experimental data from Ref. [15], the fraction p of Cd atoms bonded to TOPO equal to 0.60 for $D = 1.8$ nm, and $p = 0.35$ for $D = 2.8$, 4.1, and 7 nm were used. Finally, the magnetization data were corrected for the estimated mass of TOPO attached to each particle so that μ/Cd could be calculated. The above considerations were then used to derive the following equation for M_s:

$$M_s = 3\mu p/\rho a_o^2 D \quad (1)$$

The solid line in Figure 3 is drawn using Equation 1 with $\mu = 0.0075\ \mu_B$, with the other parameters noted above. The fact that a single value of μ gives a good agreement with the data for all the particles provides confidence in the analysis. M_s decreases with increase in D because the percentage of Cd atoms attached to TOPO decreases with increasing D. Because of the small value of $\mu = 0.0075\ \mu_B$ and the $1/D$ dependence, the effect of RTFM is observable only for small D. Equation 1 was recently used in connection with magnetism in capped gold nanoparticles.[21]

To rule out the possibility of Fe impurities as the source of observed ferromagnetism in CdSe QDs, we analyzed the TOPO-capped 1.8 nm and 7 nm samples by the ICP-AES technique described later under Experimental. With the precision of 0.1 ppm of this technique, no Fe impurities could be detected. Even 1 ppm of Fe, if present, would yield a $M_s = 1.7 \times 10^{-3}$ emu cm^{-3} (using $M_s = 1700$ emu cm^{-3} for Fe), compared to $M_s = 0.283$ emu cm^{-3} (or $M_s = 0.05$ emu g^{-1}) observed for the 1.8 nm CdSe sample. If oxides of Fe

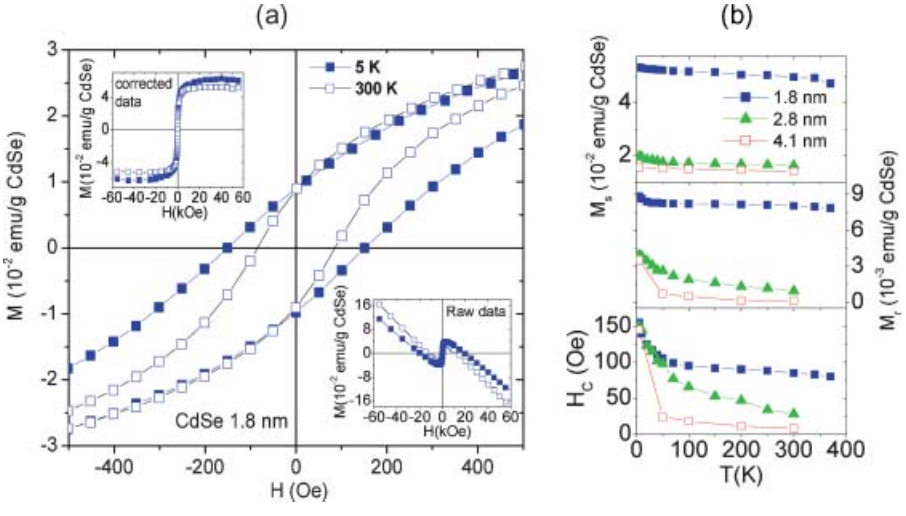

Figure 1. a) Hysteresis loops observed in 1.8 nm CdSe at 5 K and 300 K. The insets show the raw data (bottom right) and the data after subtracting the high-field diamagnetic component (top left). b) Temperature dependence of the saturation magnetization M_s, remanance M_r and coercivity H_c for the 1.8, 2.8, and 4.1 nm CdSe samples.

 © 2008 WILEY-VCH Verlag GmbH & Co. KGaA, Weinheim

ADVANCED MATERIALS

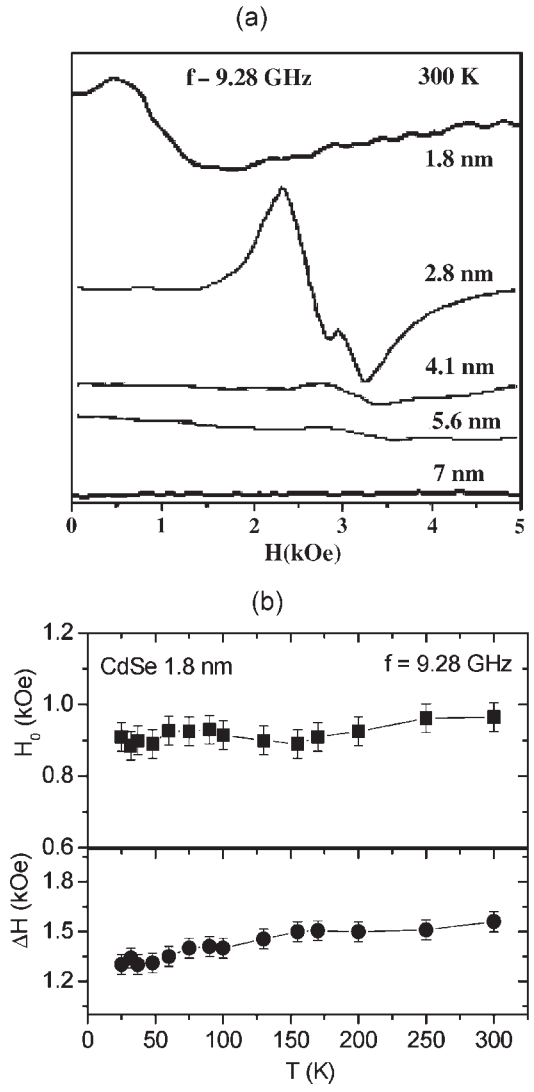

Figure 2. a) Standard derivative EMR spectra for the 1.8, 2.8, 4.1, 5.6, and 7 nm CdSe at room temperature. b) Temperature variation of the resonance field H_0 and linewidth ΔH of the EMR line for the 1.8 nm CdSe.

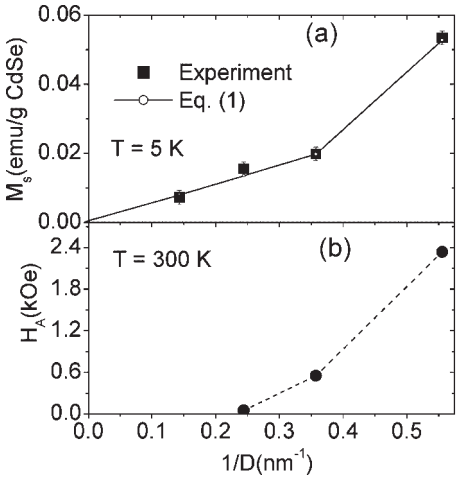

Figure 3. Dependence of the a) saturation magnetization M_s and b) anisotropy H_A (determined from the resonance field H_0) on $1/D$. The solid line represents Equation 1 and the dotted line connecting the point is for visual aid.

such as Fe_3O_4 or γFe_2O_3 ($M_s = 390\,\mathrm{emu\,cm^{-3}}$) in quantities $\simeq$1 ppm were the source for ferromagnetism, then $M_s = 0.39 \times 10^{-3}\,\mathrm{emu\,cm^{-3}}$ would be expected. Since these estimates of M_s, based on an even more generous level of 1 ppm of impurities, are at least two orders of magnitudes smaller the observed values, these impurities as sources for the observed ferromagnetism can be ruled out. Besides, it is not possible to explain the observed size dependence of M_s if same levels of impurities are assumed in all the samples.

The mechanism of charge transfer from Cd to TOPO invoked in our interpretation was measured in some of our samples using XANES (X-ray absorption near-edge structure) and EXAFS (extended X-ray absorption fine structure) spectra of TOPO-capped CdSe QDs. Whereas XANES provides element specific information of the electronic structure, EXAFS is the absorption spectra beyond the XANES region providing information of local environment around the absorbing atom such as the type of neighboring atoms, coordination number and bond lengths.

Figure 4a presents the Cd K-edge XANES spectra of CdSe QDs after background correction. The absorption feature measures the number of unoccupied states above the Fermi level. The data show an increase in the peak intensity with size reduction suggesting an increase in the number of unoccupied states and an increasing charge loss in the occupied states of Cd ion with decreasing size. On the surface of the nanoparticles, Cd with electronegativity of 1.69 is surrounded by Se with electronegativity of 2.55 and oxygen atom from TOPO (inset of Fig. 4a) with even higher electronegativity of 3.44. This additional charge transfer to Se in CdSe QDs results in the decrease in the lattice constant with decreasing size[1,2] and even more charge transfer to oxygen of TOPO. Experimental evidence for the latter comes from the EXAFS results discussed next.

The local structure around the Cd atoms is represented by the Fourier transfer (FT) of the EXAFS $k^2\chi$ data at the Cd K-edge (Fig. 4b), with the inset showing the Cd-K-edge $k^2\chi$ EXAFS oscillations for bulk CdSe and the 2.8, 4.1, and 5.6 nm QDs. The weaker intensity of the oscillation for the smaller sizes indicates more disordered local structure. In the FTs, the decrease in the amplitude of the peak near 2.27 Å due to Cd–Se bond length with decreasing size indicates reduction of the coordination number of Cd and increase of the local disorder. The additional feature on the low energy side (shown by the arrow in Fig. 4b) is due to Cd–O bond for the smaller QDs since it is known that Cd–O is shorter by about 0.2 Å than Cd–Se distance.[22] These observations thus strongly support the assumption of charge transfer between Cd and oxygen depicted schematically in Figure 4a. This charge transfer would deplete the $4d^{10}$ otherwise full band of Cd, creating holes and producing a net magnetic moment for Cd atoms bonded to

© 2008 WILEY-VCH Verlag GmbH & Co. KGaA, Weinheim

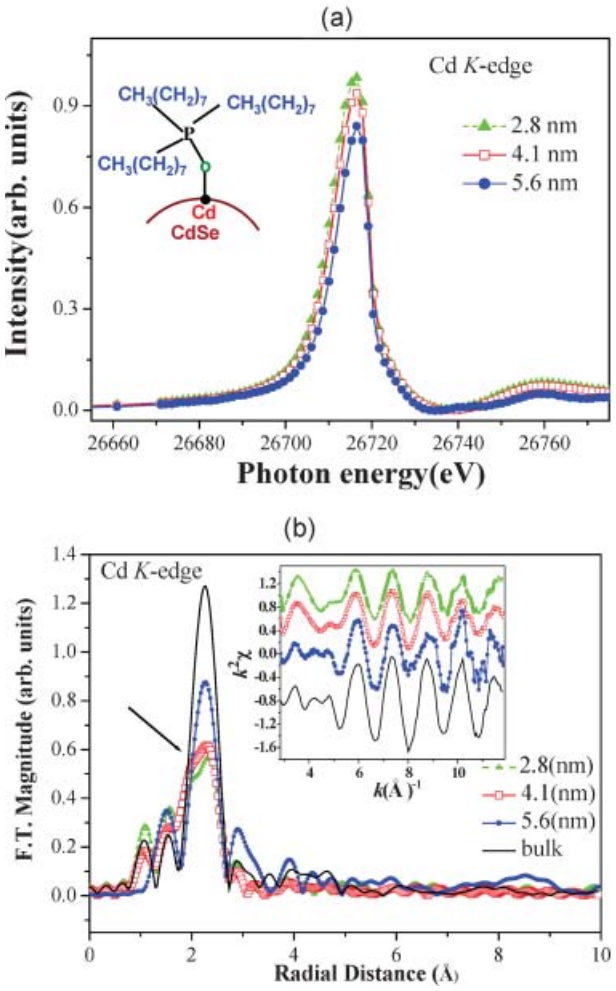

Figure 4. a) Normalized Cd K-edge XANES spectra of CdSe for 2.8 nm, 4.1 nm, and 5.6 nm nanoparticles after background subtraction. The inset shows a model of surface Cd atoms binding to TOPO molecule. b) Fourier transforms amplitudes of the EXAFS $k^2\chi$ data at the Cd K-edge for 2.8 nm, 4.1 nm, 5.6 nm, and bulk CdSe. The inset represents $k^2\chi$ data of the Cd K-edge EXAFS oscillations.

TOPO on the surface of the CdSe QDs. Since the Cd:Se stoichiometry on the surface becomes larger than one with decreasing size,[23] Equation 1 derived earlier showing M_s varying as $1/D$ follows.

The results and associated arguments presented above have shown that with reduction in size D of the CdSe QDs, an increase in the d-hole population of the Cd 4d band is possible as a result of the charge redistribution with the capping agent TOPO. These arguments lead to the saturation magnetization varying as $1/D$, in agreement with the observations reported here. In further support of our analysis, it is noted that somewhat similar effects of ferromagnetism and charge transfer have also been reported in metallic system of capped-gold nanoparticles,[24,25] where similar mechanism of d-hole ferromagnetism has been reasonably well established through a series of additional experiments. For example, although the naked NCs of Au with $D = 4$ nm only showed paramagnetism,[26] the capped Au NCs showed ferromagnetism with the saturation magnetization M_s depending strongly on the capping agent.[25] Furthermore, direct observation of ferromagnetic spin polarization on Au NCs of $D = 1.9$ nm has been measured using X-ray magnetic circular dichroism (XMCD).[27] Our observation of similar effects of size-dependent charge redistributions with the capping agent, but now in the semiconductor system of CdSe QDs as described above, represents further extension of these concepts to a new class of materials viz. semiconductors. Experiments using XMCD and with different capping agents on CdSe QDs remain to be carried out to further verify and establish these concepts. The increase in anisotropy with decrease in size D of CdSe QDs observed here (Fig. 3) is also somewhat similar to the observation reported in Au NCs,[28] the later interpreted in terms of the effects of spin-orbit interaction at the surface. This enhanced anisotropy may be sufficient to stabilize the ferromagnetic order without the need for the usual exchange coupling. As noted earlier here for CdSe QDs, not all surface Cd atoms are bonded to TOPO even for the smallest D[15,20] so that uneven bonding at the surface could also be the source of the anisotropy observed in Figure 3.

In summary, the observed size-dependent ferromagnetism in TOPO-capped CdSe QDs reported here is convincingly intrinsic. Arguments have been presented that this ferromagnetism is due to d-holes on the Cd site bonded to TOPO created by experimentally observed charge transfer from Cd to TOPO. Experiments using different capping agents and direct observation of spin polarization at the Cd site using X-ray magnetic circular dichroism would provide additional support for the mechanism of size-dependent ferromagnetism suggested in this work.

Experimental

CdSe QDs were prepared from the pyrolysis of dimethylcadmium ($Cd(CH_3)_2$, Alfa) and tri-*n*-octylphosphine selenide (TOPSe, prepared by dissolving Se shot in TOP, Aldrich) in a hot coordinating solvent of tri-*n*-octylphosphine oxide (TOPO, Aldrich) using the known procedure described previously by Murray et al. [29]. Different sizes of quantum dots were obtained by controlling its nucleation and growth process. For further size selection, size-selective precipitation can be carried out in a chloroform/methanol solvent system. The sizes of the QDs were deduced from the exciton peaks of the absorption spectra (HP 8452 diode array spectrophotometer) [30] and observed by the high-resolution TEM analysis with an accelerating voltage of 200 keV (JEM-2100, JEOL). The different sizes of QDs prepared with diameter of 1.8, 2.8, 4.1, 5.6 and 7 nm with a standard deviation of ~10% were determined. The X-ray diffraction patterns of the QDs were recorded using a 3-KW Philips diffractometer equipped with an array detector based on real time multiple strip.

The chemical analysis (ICP-AES) was carried out by a JOBIN YVON EMISSION JY24. The blank solution including 1% aqua regia (aqua regia is manufactured by trace analysis grade HCl and HNO_3, MERCK) was prepared first. 1.8 nm and 7 nm CdSe QDs were dissolved in a.u. regia, and then these samples were diluted to 1% by water (18 MΩ). In first, the calibration curve relating to iron concentration was determined by ICP-AES instrument. Correlation

 © 2008 WILEY-VCH Verlag GmbH & Co. KGaA, Weinheim

ADVANCED MATERIALS

coefficient (the *R* value) of this curve is 0.9997. The iron percentage in CdSe QDs could be detected quantitatively by using this calibration curve.

Measurements of magnetization (*M*) versus applied field *H* and temperature *T* were carried out using a commercial SQUID (superconducting quantum interference device) magnetometer (MPMS, Quantum Design). The sample was kept in a piece of white plastic straw during measurements. For all the samples, the magnetization data were corrected for the diamagnetic signal from the straw. EMR (electron magnetic resonance) response of the samples was investigated using a conventional reflection-type spectrometer operating at 9.28 GHz and using a variable temperature (5–300 K) cryostat. A high purity quartz tube was used as the sample holder. There was no observable EMR signal for the empty tube even at 5 K. The XANES and EXAFS measurements were carried out at the National Synchrotron Radiation Center in Hsinchu, Taiwan.

Received: September 19, 2007
Revised: December 1, 2007
Published online: April 15, 2008

[1] H. Ohno, *Science* **1998**, *281*, 951.
[2] T. Dietl, H. Ohno, F. Matsukura, J. Cibert, D. Ferrand, *Science* **2000**, *287*, 1019.
[3] L. M. Sandratskii, P. Bruno, *Phys. Rev. B* **2003**, *67*, 214402.
[4] A. H. Macdonald, P. Schiffer, N. Samarth, *Nat. Mater.* **2005**, *4*, 195.
[5] K. Ando, *Science* **2006**, *312*, 1883.
[6] W. K. Park, R. J. Ortega-Hertogs, J. S. Moodera, A. Punnoose, M. S. Seehra, *J. Appl. Phys.* **2002**, *91*, 8093.
[7] S. R. Shinde, S. B. Ogale, J. S. Higgins, H. Zheng, A. J. Millis, V. N. Kulkarni, R. Ramesh, R. L. Greene, T. Venkatesan, *Phys. Rev. Lett.* **2004**, *92*, 166601.
[8] L.-H. Ye, A. J. Freeman, *Phys. Rev. B* **2006**, *73*, 081304(R).
[9] A. Manivanan, G. Glaspell, P. Dutta, M. S. Seehra, *J. Appl. Phys.* **2005**, *97*, 10D325.
[10] K. Ueda, H. Tabata, T. Kawai, *Appl. Phys. Lett.* **2001**, *79*, 988.
[11] A. N. Spaldin, *Phys. Rev. B* **2004**, *69*, 125201.
[12] K. R. Kittelstved, N. S. Norberg, D. R. Gamelin, *Phys. Rev. Lett.* **2005**, *94*, 147209.
[13] P. V. Radovanovic, D. R. Gamelin, *Phys. Rev. Lett.* **2003**, *91*, 157202.
[14] S. Kuroda, N. Nishizawa, K. Takita, M. Mitome, Y. Bando, K. Osuch, K. T. Dietl, *Nat. Mater.* **2007**, *6*, 440.
[15] J. E. Bowen Katari, V. L. Colvin, A. P. Alivisatos, *J. Phys. Chem.* **1994**, *98*, 4109.
[16] S. Neeleshwar, C. L. Chen, C. B. Tsai, Y. Y. Chen, C. C. Chen, S. G. Shyu, M. S. Seehra, *Phys. Rev. B* **2005**, *71*, 201307(R).
[17] D. Magana, S. C. Perera, A. G. Harter, N. S. Dalal, G. F. Strouse, *J. Am. Chem. Soc.* **2006**, *128*, 2931.
[18] M. G. Bawendi, W. L. Wilson, L. Rothberg, P. J. Carroll, T. M. Jedju, M. L. Steigerwald, L. E. Brus, *Phys. Rev. Lett.* **1990**, *65*, 1623.
[19] M. Califano, A. Franceschetti, A. Zunger, *Nano Lett.* **2005**, *5*, 2360.
[20] G. Rafeletos, S. Norager, P. O'Brien, *J. Mater. Chem.* **2001**, *11*, 2542.
[21] P. Dutta, S. Pal, M. S. Seehra, M. Anand, C. B. Roberts, *Appl. Phys. Lett.* **2007**, *90*, 213102.
[22] K. Moller, M. M. Eddy, G. D. Stucky, N. Herron, T. Bein, *J. Am. Chem. Soc.* **1989**, *111*, 2564.
[23] J. Taylor, T. Kippeny, S. J. Rosenthal, *J. Clust. Sci.* **2001**, *12*, 571.
[24] P. Zhang, T. K. Sham, *Phys. Rev. Lett.* **2003**, *90*, 245502.
[25] H. Hori, Y. Yamamoto, T. Iwamoto, T. Miura, T. Teranishi, M. Miyake, *Phys. Rev. B* **2004**, *69*, 174411.
[26] W.-H. Li, S. Y. Wu, C. C. Yang, S. K. Lai, K. C. Lee, H. L. Huang, H. D. Yang, *Phys. Rev. Lett.* **2002**, *89*, 135504.
[27] Y. Yamamoto, T. Miura, M. Suzuki, N. Kawamura, H. Miyagawa, T. Nakamura, K. Kobayashi, T. Teranishi, H. Hori, *Phys. Rev. Lett.* **2004**, *93*, 116801.
[28] A. Hernando, P. Grespo, M. A. Garcia, *Phys. Rev. Lett.* **2006**, *96*, 057206.
[29] C. B. Murray, D. J. Norris, M. G. Bawendi, *J. Am. Chem. Soc.* **1993**, *115*, 8706.
[30] C. D. Dushkin, S. Saita, K. Yoshie, Y. Yamaguchi, *Adv. Colloid Interface Sci.* **2000**, *88*, 37.

© 2008 WILEY-VCH Verlag GmbH & Co. KGaA, Weinheim